$B^0_{d,s} \to \mu^- \mu^+$ decay in the MSSM

Piotr H. Chankowski and Łucja Sławianowska
Institute of Theoretical Physics, Warsaw University, 00-681 Warsaw, Poland
(Received 24 August 2000; published 5 February 2001)

We present the results of the complete one-loop computation of the $B^0_{d,s} \to l^+ l^-$ decay rate in the MSSM. Both sources of the FCNC, the CKM matrix and off-diagonal entries of the sfermion mass matrices are considered. Strong enhancement of the branching ratio (compared to the SM prediction) can be obtained in the large $\tan\beta \sim m_t/m_b$ regime in which the neutral Higgs boson ''penguin'' diagrams dominate. We make explicit the strong dependence of this enhancement on the top squarks mixing angle in the case of the chargino contribution and on the μ parameter in the case of the gluino contribution. We show that, in some regions of the MSSM parameter space, the branching ratio for this process can be as large as $10^{-(5-4)}$ respecting all existing constraints, including the CLEO measurement of $\mathrm{BR}(B \to X_s \gamma)$. We also estimate that for chargino and top squark masses $\sim \mathcal{O}(100\ \mathrm{GeV})$ $\mathrm{BR}(B^0_s \to l^+ l'^-)$ with $ll' = e\tau$ or $\mu\tau$ can be of the order of 10^{-11} for the still allowed values of the off-diagonal entries in the slepton mass matrix.

DOI: 10.1103/PhysRevD.63.054012 PACS number(s): 13.20.He, 12.15.Ji, 12.15.Mm, 12.60.Jv

I. INTRODUCTION

Extensions of the standard model (SM) usually predict new contributions to the flavor changing neutral current (FCNC) processes. For example, adding in the most general way a second doublet of the Higgs fields to the standard theory of electroweak interactions typically leads to large amplitudes of FCNC processes mediated at the tree level by neutral Higgs particles. Restricting appropriately the possible form of couplings of the two Higgs doublets to up- and down-type fermions eliminates such tree level contributions to FCNC processes, but, of course, new contributions induced by loops involving the physical charged scalar still remain. Charged Higgs boson contributions to FCNC processes depend however on the same elements of the Cabibbo-Kobayashi-Maskawa (CKM) mixing matrix as does the standard $W^\pm$ boson contribution and, thus, amplify the effects of the FCNC source that is present in the SM, rather than being an independent new source of such processes. Nevertheless, requiring the effects of the charged Higgs boson not to spoil successful predictions of the standard theory leads to interesting bounds on the $(M_{H^+}, \tan\beta)$ plane, where $\tan\beta \equiv v_2/v_1$ is the ratio of the vacuum expectation values of the two Higgs doublets. In particular, in the popular two Higgs doublet model of type II (2HDMII), in which the first doublet couples only to leptons and down-type quarks and the second one couples to up-type quarks only, processes such as $B \to X_s \gamma$ and $K^0 \overline{K^0}$ mixing together with $Z^0 \to \overline{b}b$ constrain the plane $(M_{H^+}, \tan\beta)$. In particular, for $\tan\beta \gtrsim 3$ $B \to X_s \gamma$ requires $H^\pm$ to be heavier than $\sim 165-200$ GeV [1].

Supersymmetric models, such as the minimal supersymmetric standard model (MSSM), which are the most popular and best motivated extensions of the SM, apart from containing a charged Higgs boson $H^\pm$, induce additional contributions to the FCNC processes. Firstly, in such models the effects of the CKM mixing can be further amplified through the loops involving charginos and squarks. Secondly, as there is no reason why the squark mass matrices should be diagonal in the same (so-called super-CKM) basis as quarks, the sfermion sector of such models is, in general, a new, independent of the CKM matrix, source of the FCNC processes.

Current experimental data on FCNC processes provide important constraints on these sources of flavor nonconservation in supersymmetric models. (Extensive reviews are Refs. [2] and [3].) Taking the CKM matrix as the only source of the FCNC processes, the current experimental data on $B \to X_s \gamma$ and $K^0 \overline{K^0}$, $B^0 \overline{B^0}$ mixings impose some constraints on the MSSM parameter space. These constraints, which correlate masses and composition of charginos and top squarks with the mass of the charged Higgs boson, depend in part on the element V_{td} of the CKM matrix, which is not directly measured [3,4], and become weaker with growing sparticle masses. Effects of the nonzero off-diagonal entries of the sfermion mass matrices are usually analyzed separately [2,3]. Stringent constraints apply to the entries causing transitions between the first two generations. Bounds on the entries connected to the third generation, which follow from the $B^0 \overline{B^0}$ mixing and $B \to X_s \gamma$ decay are much weaker. Thus large deviations from the rates predicted in the SM can still be discovered in the forthcoming (or already running) experiments such as BaBar (SLAC), BELLE (KEK), CLEO (Cornell), HERA-B (DESY) and the Large Hadron Collider (LHC) (CERN). In this context, a particularly interesting process to look at are the decays $B^0_{s(d)} \to l^+ l^-$ because they are clean, theoretically being almost free of hadronic uncertainties.

Several papers analyzed this process in the MSSM [5–7] under various assumptions and with different approximations. In this paper, we perform a complete calculation[1] of the process $B^0_{s,d} \to l^- l^+$ in the MSSM with emphasis on

[1] In what follows we display only formulas for the dominant contributions. The plots are, however, based on the program including contributions from all relevant one-loop diagrams.

qualitative understanding of the dominant effects. To this end we derive simple analytical formulas approximating the main contributions. We reconfirm that for values of $\tan\beta < 20$ the rate of this process is not significantly enhanced compared to the prediction of the SM [apart from the case of $\tan\beta \sim 0.5$ and light $H^{\pm}$ [8] which is not favored theoretically within the supersymmetric framework and in which the effects are severely limited by the measured $B \to X_s\gamma$ rate and $R_b \equiv \Gamma(Z^0 \to \bar{b}b)/\Gamma(Z^0 \to \text{hadr})$]. In agreement with earlier papers [6], we find that large enhancement of the branching ratio is obtained in the case of large $\tan\beta$ values due the neutral Higgs boson penguin graphs. This has been previously made explicit in Ref. [7] (a possible role of such contributions to K^0-$\bar{K}^0$ and B^0-$\bar{B}^0$ mixing has been emphasized in Ref. [9]) in which the contributions of charginos as a source of the flavor changing has been considered. We demonstrate strong dependence of the decay rate on the value of the top squark mixing angle and explain it using our analytic formulas. Moreover, we extend previous calculations by also analyzing the case of the flavor mixing induced by squark mass matrices. In the latter case, we find very strong dependence on the μ parameter. Finally, we correlate the predictions for $B^0_{s,d} \to l^- l^+$ with the constraints imposed on the parameter space by other processes, in particular, by the measurement by CLEO [10] of the $B \to X_s\gamma$ branching ratio. We find that even respecting all those constraints, $\mathrm{BR}(B^0_s \to \mu^-\mu^+)$ can be enhanced up to $10^{-(4-5)}$ for $\tan\beta \sim m_t/m_b \approx 50$. Moreover, for such values of $\tan\beta$ and the off-diagonal 13 entries of the down-type squark mass matrix saturating the existing bound [2,3], also $\mathrm{BR}(B^0_d \to \mu^-\mu^+)$ can be of the same order of magnitude. This means that the unsuccessful search done at CLEO [11] already provides a constraint on the 13 off-diagonal entries of the down-type squarks which, for some values of the other MSSM parameters, is stronger than the one given in Refs. [2,3]. Finally, we also estimate that for chargino and top squark masses $\sim \mathcal{O}(100\ \mathrm{GeV})$ $B^0_s \to l^+ l'^-$ with $ll' = e\tau$ or $\mu\tau$ can be of order 10^{-11} for the still allowed values of the off-diagonal entries in the slepton mass matrix.

II. GENERAL STRUCTURE OF THE AMPLITUDE AND THE SM PREDICTION

The effective Lagrangian describing the $d_I\bar{d}_J \to \bar{l}_A l_B$ transition has the general form

$$\mathcal{L}_{eff} = \sum_x C_x \mathcal{O}_x \tag{1}$$

in which $\mathcal{O}_x$ are the local four-fermion operators and C_x are their Wilson coefficients (we suppress quark and lepton flavor indices on $\mathcal{O}_x$ and C_x, as well as on various form factors which will appear in the following). Four vector-vector operators $\mathcal{O}^V_{XY} \equiv (\bar{d}_J\gamma_\mu P_X d_I)(\bar{l}_B\gamma^\mu P_Y l_A)$ and four scalar operators $\mathcal{O}^S_{XY} \equiv (\bar{d}_J P_X d_I)(\bar{l}_B P_Y l_A)$ (where $X,Y = LL, RR, LR$ and RL) contribute to this process. In addition, two tensor operators exist but they do not contribute to this process (their matrix elements vanish when taken between one meson and vacuum states). In the following, we will specify the formulas to the case of $B^0_{d(s)} = \bar{b}d(s)$ decay; hence we will take $J=3$ and $I=1=d$ for B^0_d or $I=2=s$ for B^0_s. Furthermore, because of the pseudoscalar nature of the B^0_I mesons, we need only two matrix elements:[2]

$$\langle 0|\bar{b}\gamma^\mu\gamma^5 d_I|B^0_I(q)\rangle = -if_{B_I}q^\mu,$$
$$\langle 0|\bar{b}\gamma^5 d_I|B^0_I(q)\rangle = +if_{B_I}\frac{M_B^2}{m_{d_I}+m_b}. \tag{2}$$

Using Eq. (2) one finds the total B^0 width

$$\Gamma = \frac{M_B}{16\pi} f(x_A^2, x_B^2)\{|a|^2[1-(x_A-x_B)^2] + |b|^2[1-(x_A+x_B)^2]\}, \tag{3}$$

where $f(x,y) \equiv \sqrt{1-2(x+y)+(x-y)^2}$, $x_A \equiv m_{l_A}/M_B$ and the coefficients a and b are given in terms of the Wilson coefficients as

$$a = \frac{f_{B_I}}{4}\left\{(m_{l_B}+m_{l_A})[C^V_{LL}-C^V_{LR}+C^V_{RR}-C^V_{RL}] - \frac{M^2_{B_I}}{m_b}[C^S_{LL}-C^S_{LR}+C^S_{RR}-C^S_{RL}]\right\}, \tag{4}$$

$$b = -\frac{f_{B_I}}{4}\left\{(m_{l_B}-m_{l_A})[C^V_{LL}+C^V_{LR}-C^V_{RR}-C^V_{RL}] - \frac{M^2_{B_I}}{m_b}[C^S_{LL}+C^S_{LR}-C^S_{RR}-C^S_{RL}]\right\}, \tag{5}$$

where we have neglected m_{d_I} compared to m_b.

Three groups of diagrams contribute to the Wilson coefficients: box diagrams, Z^0 penguin diagrams, and neutral Higgs boson penguin diagrams.[3] Denoting the self-energy diagrams on the external quark lines as $-i\Sigma(\not{p})$, with

$$\Sigma(\not{p}) = \Sigma^V_L\not{p}P_L + \Sigma^V_R\not{p}P_R + \Sigma^S_L P_L + \Sigma^S_R P_R, \tag{6}$$

and vertex corrections to the couplings $\bar{d}_J d_I Z^0$, $\bar{d}_J d_I S^0$ and $\bar{d}_J d_I P^0$, where $S^0(P^0)$ is a neutral scalar (pseudoscalar), respectively, as

[2]The second follows from the first one by using the QCD equation of motion for the quark field operators; this fixes their relative sign.

[3]At the one-loop level the photon penguin diagram does not contribute for the $\bar{l}l$ final state due to the vector current conservation. As long as neutrinos are massless, the $\bar{l}l'$ final state can appear neither in the SM nor in the 2HDM; in the MSSM, the $\bar{l}l'$ final state can only be due to box contribution, provided the slepton mass matrices remain nondiagonal in the lepton mass eigenstate basis.

$$+i\gamma^\mu(F_L^V P_L+F_R^V P_R)$$
$$-i(F_L^S P_L+F_R^S P_R)$$
$$-(F_L^P P_L+F_R^P P_R), \tag{7}$$

one finds [in the approximation $\Sigma(p^2)\equiv\Sigma(0)$, $F(q^2)=F(0)$] the following expressions for the Wilson coefficients generated by various penguin diagrams:

$$C_{XY}^V=-\frac{e}{2s_W c_W M_Z^2}\hat{F}_X^V c_Y^e,\quad X,Y=L,R \tag{8}$$

from the Z^0 penguin diagram, with $c_L^e=1-2s_W^2$, $c_R^e=-2s_W^2$, and s_W (c_W) is the sine (cosine) of the Weinberg angle,

$$C_{LL}^S=C_{LR}^S=\sum_{k=1,2}\frac{1}{M_{H_k^0}^2}\frac{Z_R^{1k}}{v_1}\hat{F}_L^S m_l,$$
$$C_{RR}^S=C_{RL}^S=\sum_{k=1,2}\frac{1}{M_{H_k^0}^2}\frac{Z_R^{1k}}{v_1}\hat{F}_R^S m_l \tag{9}$$

from neutral scalar penguin diagrams, and

$$C_{LL}^S=-C_{LR}^S=\sum_{k=1,2}\frac{1}{M_{H_{k+2}^0}^2}\frac{Z_H^{1k}}{v_1}\hat{F}_L^P m_l,$$
$$C_{RR}^S=-C_{RL}^S=\sum_{k=1,2}\frac{1}{M_{H_{k+2}^0}^2}\frac{Z_H^{1k}}{v_1}\hat{F}_R^P m_l \tag{10}$$

from neutral pseudoscalar penguin diagrams. We use here (and throughout) the notation of Ref. [12] in which $H_k^0\equiv(h^0,H^0)$, $H_{2+k}^0\equiv(A^0,G^0)$, $H_k^\pm\equiv(H^\pm,G^\pm)$ and Z_R^{1k} (Z_H^{1k}) denote the projection of the kth physical neutral CP-even (-odd) Higgs boson onto the real (imaginary) part of the neutral component of the Higgs doublet that couples to the down-type quarks. In addition, since at one loop penguin graphs cannot generate transitions $B^0\to\bar{l}l'$, we have set $m_{l_A}=m_{l_B}=m_l$. In these formulas,

$$\hat{F}_{L,R}^V=F_{L,R}^V+\frac{e}{2s_W c_W}c_{L,R}^d\Sigma_{L,R}^V, \tag{11}$$

where $c_L^d=1-2s_W^2/3$, $c_R^d=-2s_W^2/3$,

$$\hat{F}_{L,R}^S=F_{L,R}^S-\frac{Z_R^{1k}}{v_1}\Sigma_{L,R}^S, \tag{12}$$

and

$$\hat{F}_L^P=F_L^P+\frac{Z_H^{1k}}{v_1}\Sigma_L^P,\quad \hat{F}_R^P=F_R^P-\frac{Z_H^{1k}}{v_1}\Sigma_R^S \tag{13}$$

are the full effective vertices, including the effects of flavor changing self-energy diagrams on the external quark lines. Box diagram contributions to the Wilson coefficients can also be easily found. From Eqs. (4), (5), and (8)–(10), one sees that scalar penguin diagrams contribute only to b in Eq. (3), whereas the coefficient a receives contributions from both Z^0 and the pseudoscalar penguin diagrams. The relative sign of the Z^0 and the neutral Goldstone boson contributions to a should be such that the total contribution is independent of the gauge chosen for the Z^0 propagator. This is the case if

$$-m_J\hat{F}_{L,R}^V+m_I\hat{F}_{R,L}^V=-M_Z\hat{F}_{L,R}^P \tag{14}$$

for P referring to the Goldstone boson. Since the form factor $\hat{F}_{L,R}^P$ for the physical pseudoscalar A^0 is related to the one for G^0 by the $SU_L(2)$ symmetry, this relation tests also the relative sign of the Z^0 and pseudoscalar penguin diagrams.

The SM contribution to the $B^0\to ll$ decay is well known [13] (see, also, Ref. [14]). The Higgs boson couplings to fermions are not enhanced, so the scalar and pseudoscalar penguins are negligibly small. The only important box diagram is the one with two $W^\pm$ which contributes only to C_{LL}^V

$$C_{LL}^V=-\frac{1}{16\pi^2}\left(\frac{e}{s_W}\right)^4\frac{\lambda_{tI}}{M_W^2}\frac{x_t}{4}\left[\frac{1}{1-x_t}+\frac{\log x_t}{(1-x_t)^2}\right], \tag{15}$$

where $x_t\equiv(m_t/M_W)^2$ and $\lambda_{tI}\equiv V_{tJ}^\star V_{tI}$. The effective $\bar{d}_J d_I Z^0$ vertex receives contributions from loops involving both $W^\pm$ and the charged Goldstone bosons. One finds

$$\hat{F}_L^V=\frac{1}{16\pi^2}\frac{e^3}{4s_W^3 c_W}\lambda_{tI}x_t\left[\frac{x_t-6}{1-x_t}-\frac{3x_t+2}{(1-x_t)^2}\log x_t\right] \tag{16}$$

and $\hat{F}_R^V=0$ in the limit of $m_{d_I}=0$. Adding all one gets

$$\mathrm{BR}(B_I^0\to\bar{l}l)=\tau(B_I^0)\times\left[\frac{G_F\alpha}{4\pi s_W^2}\right]^2\frac{f_{B_I}^2 m_l^2 M_{B_I}}{\pi}|\lambda_{tI}|^2\sqrt{1-4\frac{m_l^2}{M_{B_I}^2}}Y_0^2(x_t), \tag{17}$$

where $\tau(B_I^0)$ is the lifetime of the B_I^0 meson and [15,14]

$$Y_0(x_t)=-\frac{x_t}{8}\left[\frac{x_t-4}{x_t-1}+\frac{3x_t}{(x_t-1)^2}\log x_t\right]. \tag{18}$$

In general, taking QCD corrections into account consists of computing corrections to the Wilson coefficients at the scale $\sim M_Z$, and subsequently evolving the latter from the electroweak scale down to the hadronic scale $\mu_h\sim m_b$. The first step of this procedure amounts to replacing $Y_0(x_t)$ by $Y(x_t)=Y_0(x_t)+(\alpha_s/4\pi)Y_1(x_t)$ [15], where now $x_t=(\overline{m}_t(m_t^2)/M_W)^2$. $Y(x_t)$ can be conveniently parametrized as [16]

$$Y(x_t)=0.997\left[\frac{\overline{m}_t(m_t)}{166\ \mathrm{GeV}}\right]^{1.55}.$$

As far as the evolution is concerned, it has been noted in Ref. [16] that the vector operators contributing to $B^0\to\overline{l}l$ have zero anomalous dimensions. Hence, their Wilson coefficients do not evolve at all, whereas the evolution of the Wilson coefficients of the scalar operators result in multiplying them by $m_b(\mu_h)/m_b(M_Z)$. Consequently, if C^S_{XY} are proportional to $m_b(M_Z)$, their evolution is taken into account if this factor is replaced by $m_b(\mu_h)$, which in turn cancels out with the factor $1/m_b(\mu_h)$ present in Eqs. (4) and (5). As it will be apparent, whenever the coefficients C^S_{XY} are large, they are indeed proportional to $m_b(M_Z)$. In the SM, including QCD corrections, one finds [16]

$$\mathrm{BR}(B_s^0\to\overline{\mu}\mu)=4.1\times10^{-9}\left[\frac{\tau(B_s)}{1.54\ \mathrm{ps}}\right]\times\left[\frac{f_{B_s}}{245\ \mathrm{MeV}}\right]^2\left[\frac{|V_{ts}|}{0.040}\right]^2\left[\frac{\overline{m}_t(m_t)}{166\ \mathrm{GeV}}\right]^{3.12}. \quad (19)$$

III. CONTRIBUTION OF THE EXTENDED HIGGS SECTOR

As remarked in the Introduction, the presence of the physical charged Higgs boson in the extended Higgs sector of the MSSM (or 2HDM), in general, enhances the FCNC transition rates generated by the CKM mixing matrix. This enhancement can appear through the $H^\pm$ contribution to box diagrams, Z^0 penguin diagrams and neutral Higgs boson penguin diagrams. The latter type of diagrams can only be important in the large $\tan\beta\gtrsim30$ regime in which the neutral Higgs boson couplings to the down-type quarks and charged leptons are enhanced by $\tan\beta$ factors.

For low values of $\tan\beta\lesssim20$, the neutral Higgs boson penguin diagrams are small. It is also easy to check that for such $\tan\beta$ values no box diagram can give significant contribution. Thus the only large contribution can be due to the $H^\pm$ contribution to the Z^0 penguin diagrams. Computing the relevant self-energy diagrams (vector parts thereof) and vertex corrections, one arrives at

$$\Delta\hat{F}_L^V=\frac{1}{16\pi^2}\frac{e^3}{(s_Wc_W)^3}\lambda_{tI}\cot^2\beta\frac{m_t^2}{M_Z^2}\frac{1}{4}\frac{y_t}{1-y_t}\times\left[1+\frac{1}{1-y_t}\log y_t\right],$$

$$\Delta\hat{F}_R^V=-\frac{1}{16\pi^2}\frac{e^3}{(s_Wc_W)^3}\lambda_{tI}\tan^2\beta\frac{m_bm_{d_I}}{M_Z^2}\frac{1}{4}\frac{y_t}{1-y_t}\times\left[1+\frac{1}{1-y_t}\log y_t\right],$$

where $y_t\equiv(m_t/M_{H^+})^2$. Taking into account only $\Delta\hat{F}_L^V$, which is enhanced for $\tan\beta<1$, amounts to replacing $Y(x_t)$ in Eq. (17) by

$$Y(x_t)\to Y(x_t)-\cot^2\beta\frac{x_t}{8}\frac{y_t}{1-y_t}\left[1+\frac{1}{1-y_t}\log y_t\right]. \quad (20)$$

The new contribution has the same sign as $Y(x_t)$ and, therefore, enhances the SM contribution. For example, for $\tan\beta=0.5$ and $M_{H^+}=M_W$, $\mathrm{BR}(B^0\to\overline{l}l)$ is enhanced by a factor of $(1+1.566/0.997)^2\approx6.6$ compared to the SM prediction.

For large $\tan\beta\sim m_t/m_b$ in the case of B_s^0 decay, $\hat{F}_R^V$, despite being suppressed by one power of m_s/M_W, is about two orders of magnitude larger than $\hat{F}_L^V$ and, for $M_{H^+}\sim100$ GeV, is of the order of the SM contribution. However, in this regime, there are other contributions that are more important [17,16].

First, the mixed, $W^\pm H^\pm$, box diagram in which $H^\pm$ couples to the b quark is also $\mathcal{O}(\tan^2\beta)$ and not suppressed by m_{d_I}/M_W. After summation over different types of virtual quarks it gives [16]

$$C^S_{\mathrm{LR}}=\frac{1}{16\pi^2}\left(\frac{e}{s_W}\right)^4\frac{m_lm_b}{M_W^2}\lambda_{tI}\tan^2\beta\frac{1}{4}\frac{x_t}{x_H-x_t}\times\left[\frac{1}{x_H-1}\log x_H-\frac{1}{x_t-1}\log x_t\right], \quad (21)$$

where $x_H\equiv(M_{H^\pm}/M_W)^2$. The other $W^\pm H^\pm$ box is proportional to m_{d_I}/M_W and hence it is less important. The box diagrams containing two charged scalars (either physical or Goldstone) are suppressed always by $(m_l/M_W)^2$. Therefore, although the $H^\pm H^\pm$ box grows as $\tan^4\beta$, it is not important even for $\tan\beta\sim50$.

Second, there are neutral Higgs boson penguin diagrams. It turns out [16] that the dominant, i.e., $\sim\tan\beta$ part of the genuine $\overline{d}_Jd_IS^0(P^0)$ vertex correction cancels out[4] and the only contribution arises from the scalar parts of the self-energies of external quarks (for $\overline{B}^0$ decay it is Σ_R^S which is dominant):

$$\Sigma_L^S=\frac{1}{16\pi^2}\left(\frac{e}{s_W}\right)^2m_b\lambda_{tI}x_t\frac{x_H-1}{x_H-x_t}\left[\frac{x_H}{x_H-1}\log x_H-\frac{x_t}{x_t-1}\log x_t\right], \quad (22)$$

where $x_H=(M_{H^\pm}/M_W)^2$.

Using the formulas (11) and (13), and the fact that in the MSSM for neutral CP-even scalars for large values of $\tan\beta$ the following relations hold:[5]

[4]This cancellation is even simpler in the case of the MSSM than in the case of the 2HDM(II) considered in [16].

[5]The well-known large radiative corrections to h^0 and H^0 masses do not spoil these relations. Moreover, these corrections do not affect the neutral Higgs boson penguin contributions because they always modify significantly only the mass of that Higgs boson, which almost does not couple to the down-type quarks and charged leptons.

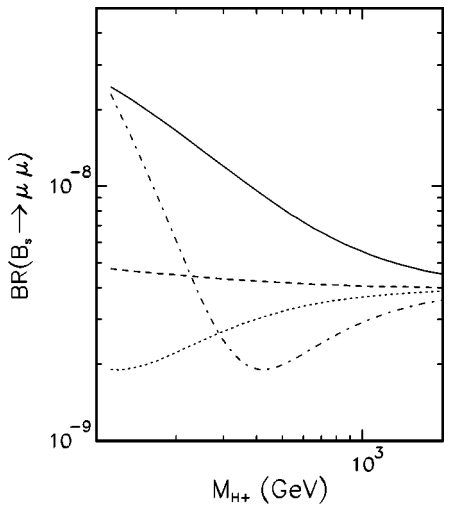

FIG. 1. Contribution of the Higgs sector of the MSSM or 2HDM(II) to BR($B^0_s\to\mu^-\mu^+$) as a function of the charged Higgs boson mass for $\tan\beta=$ 0.5 (solid line), 2 (dashed line), 25 (dotted line) and 50 (dot-dashed line).

$$\sin^2\alpha\approx 1,\ \ M_h^2\approx M_A^2 \text{ for } M_A<M_Z,$$
$$\cos^2\alpha\approx 1,\ M_H^2\approx M_A^2 \text{ for } M_A>M_Z, \tag{23}$$
$$M_{H^+}^2=M_A^2+M_W^2,$$

we can now summarize the dominant contribution of the extended Higgs sector to the coefficients a and b given by Eqs. (4) and (5), Ref. [16]:

$$a=\frac{1}{16\pi^2}\frac{f_{B_I}}{2}\left(\frac{e}{s_W}\right)^4\frac{m_l}{M_W^2}\lambda_{tI}\left[Y(x_t)-\frac{M_{B_I}^2}{8M_W^2}\tan^2\beta\frac{\log r}{r-1}\right], \tag{24}$$

$$b=-\frac{1}{16\pi^2}\frac{f_{B_I}}{2}\left(\frac{e}{s_W}\right)^4\frac{m_l}{M_W^2}\lambda_{tI}\frac{M_{B_I}^2}{8M_W^2}\tan^2\beta\frac{\log r}{r-1},$$

where $r\equiv 1/y_t=(M_{H^+}/m_t)^2$. Since $\log r/(r-1)>1$, the CP-odd neutral Higgs exchange interferes destructively with the SM contribution. Figure 1 shows the contribution of the extended Higgs sector of the MSSM (assuming that sparticles contribute negligibly) or of the 2HDM(II)[6] to BR($B^0_s\to\mu^-\mu^+$) as a function of M_{H^+} for different values of $\tan\beta$. These results, which should be compared with the SM results 4×10^{-9}, agree for $\tan\beta\gtrsim 30$ with the ones given in Ref. [16] and, for smaller values of $\tan\beta$, update the computations done earlier in Refs. [8,17]. The formulas (24) apply also to BR($B^0_d\to\mu^-\mu^+$). In this case, however, the value of the element V_{td} which for each point in the $(\tan\beta, M_{H^+})$ plane should be extracted from the data on B^0_d-$\bar{B}^0_d$ mass difference and the parameter ϵ_K, can be different than in the SM, especially for low values of $\tan\beta$. We do not attempt such an analysis here.

[6]In the case of the 2HDM(II), the subleading in $\tan\beta$ contributions of the genuine vertex corrections in the CP-even Higgs boson penguin may be different than in the MSSM, because the dimensionfull couplings $H^+H^-H^0(h^0)$ differ in both models [17]. Still, unless these couplings in the 2HDM(II) are very large (and numerically very different from their MSSM counterparts) so as to enhance the otherwise subleading contribution, Fig. 1 should be representative also for the 2HDM(II) results.

IV. CHARGINO CONTRIBUTION

Another source of amplification of the flavor changing transitions induced by the CKM matrix is the chargino sector of the MSSM. Assuming that the squark mass matrices are diagonal in the super-CKM basis, the first result is that in the whole relevant parameter space the box diagram contribution to any of the Wilson coefficients remains small compared to the SM contribution. Furthermore, the Z^0 penguin diagram can change the predicted BR($B^0_s\to\mu^-\mu^+$) by no more than $\sim$5–10% for $\tan\beta\sim 2$ and $\sim$20% for $\tan\beta\sim 0.5$. The magnitude and sign of this contribution depends, apart from the masses of the sparticles involved, also on the chargino composition and on the mixing angle of the top squarks. For natural top squark composition, i.e., when the lighter top squark is predominantly right handed and the mixing angle is not too large [18], the chargino loop contribution to the Wilson coefficients has opposite sign to that of the top quark loop and, hence, decreases the rate of the $B^0_s\to\mu^-\mu^+$ decay. This is very similar to the opposite, as compared to the SM, sign of the chargino-stop loop contribution to $R_b\equiv\Gamma(Z^0\to\bar{b}b)/\Gamma(Z^0\to\text{hadr})$ [19] since, in view of the smallness of the box contribution, the two calculations are very similar. We conclude that in the whole range of the MSSM parameter space the box and Z^0-penguin diagrams arising from chargino exchanges do not change the order of magnitude of the $B^0_s\to\mu^-\mu^+$ decay rate. (Again, to calculate the $B^0_d\to\mu^-\mu^+$ decay rate, one would have to consider the chargino contribution to the ϵ_K parameter and B^0_d-$\bar{B}^0_d$ mass difference in order to determine consistently the value of the V_{td} element.)

Huge contribution to this rate can be, however, induced for large $\tan\beta\gtrsim 30$ by neutral Higgs boson penguin diagrams. This had first been made explicit in Ref. [7] in the approach based on the effective Lagrangian method. Our numerical results are obtained by full computation of all relevant Feynman diagrams. Here we present only the derivation of the approximate formulas summarizing the dominant effects. To this end we consider the limit in which all soft SUSY breaking parameters, except for the ones which determine the Higgs potential, are much larger than the electroweak scale. In this limit, which allows us to work in the symmetric phase of the theory (i.e., with $v_i=0$) in which sfermions still have definite chirality, we can construct the effective theory by integrating out sparticles (but not the Higgs fields). In this construction, threshold corrections shown in Fig. 2 give rise to the effective Yukawa interactions of the down-type quarks summarized by

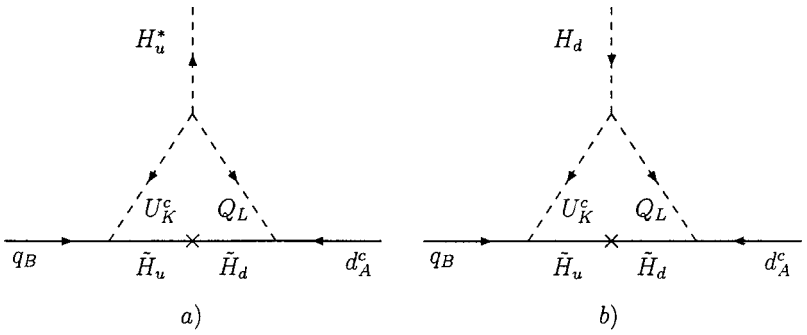

FIG. 2. Diagrams giving rise to $\Delta_u Y_d$ and $\Delta_d Y_d$, respectively, in the construction of the effective theory.

$$\mathcal{L}_{eff} = -\epsilon_{ij}(Y_d+\Delta_d Y_d)^{BA} H_i^d q_j^A d^{c\,B} - (\Delta_u Y_d)^{BA} H_i^{*u} q_i^A d^{c\,B} + \text{H.c.}, \tag{25}$$

where A and B are the generation indices and we work in the language of two-component Weyl spinors. In order to diagonalize the quark mass matrix arising after the electroweak symmetry breaking, we first perform the standard CKM rotations (diagonalizing the original matrix Y_d^{BA}) followed by the infinitesimal rotations

$$d^A \to (1+\Delta V_L^{D\dagger})^{AB} d^B, \quad d^{c\,A} \to d^{c\,B}(1+\Delta V_R^{D\dagger})^{AB}, \tag{26}$$

with $\Delta V_L^{D\dagger}$, $\Delta V_R^{D\dagger}$ satisfying $\Delta V_{L,R}^{D\dagger} = -\Delta V_{L,R}^{D}$. Diagonal mass matrix for down-type quarks is obtained with

$$-(\Delta_d' Y_d)^{AB} + \frac{v_2}{v_1}(\Delta_u' Y_d)^{AB} = (\Delta V_R^{D\dagger})^{AB} Y_d^B + Y_d^A (\Delta V_L^D)^{AB}, \tag{27}$$

where Y_d^A are already diagonal and $\Delta_{u(d)}' Y_d$ are related to the original $\Delta_{u(d)} Y_d$ by the rotation diagonalizing the original Y_d^{BA}. This leads[7] to the effective Yukawa couplings of the neutral Higgs bosons of the form

$$\mathcal{L} = -\frac{1}{\sqrt{2}} d^c(-Y_d Z_R^{1k} + \Delta_u' Y_d Z_R^{2k} - \tan\beta \Delta_u' Y_d Z_R^{1k}) d\ H_k^0 + \text{H.c.} + \frac{i}{\sqrt{2}} d^c(Y_d Z_H^{1k} + \Delta_u' Y_d Z_H^{2k} + \tan\beta \Delta_u' Y_d Z_H^{1k}) d\ H_{k+2}^0 + \text{H.c.} \tag{28}$$

[In the Lagrangian (28), Y_d is diagonal and the rest of the notation is explained below Eq. (10)] which, in general, generates the FCNC transitions. Note that the correction $\Delta_d Y_d$ disappeared altogether as it should, since it cannot contribute to the FCNC transition.

The correction $\Delta_u Y_d$ in Eq. (25) is easily computed in the basis in which Y_u^{AB} is diagonal and the initial $Y_d^{AB} = Y_d^A V_{AB}^\dagger$, where V_{AB} is the CKM matrix. Starting from the SUSY breaking part of the Lagrangian [12]

$$\mathcal{L}_{soft} = -(m_U^2)^{AB}\ U^{c*A} U^{cB} - (m_Q^2)^{AB} Q_i^{*A} Q_i^B + (\epsilon_{ij} A_U^{AB} H_u^i Q_j^A U^{cB} - \mu \epsilon_{ij} \tilde{H}_d^i \tilde{H}_u^j + \text{h.c.}),$$

we obtain

$$\Delta_u Y_d^{AB} = \frac{1}{16\pi^2} Y_d^{AC} A_U^{BC} Y_u^B \mu C_0(\mu^2, M_{Q_B}^2, M_{U_C^c}^2), \tag{29}$$

where C_0 is the standard three-point function.

$$C_0(a,b,c) = \frac{1}{a-b}\left[\frac{a}{a-c}\log\frac{a}{c} - \frac{b}{b-c}\log\frac{b}{c}\right]. \tag{30}$$

Inserting Eq. (29) in Eq. (25) and performing all steps making the usual assumption $A_U^{AB} = Y_u^A A_u^A \delta^{AB}$ (i.e., that the trilinear soft terms are proportional to the Yukawa couplings) and keeping only the top Yukawa coupling leads to

$$\Delta_u' Y_d^{JI} = \pm \frac{1}{16\pi^2} \lambda_{tI} Y_d^J Y_t^2 A_t m_{C_1} C_0(m_{C_1}^2, M_{\tilde{t}_L}^2, M_{\tilde{t}_R}^2), \tag{31}$$

where we have replaced μ with m_{C_1} and the sign $\pm$ keeps track of the sign of μ. Using Eq. (28) in Eqs. (9) ad (10) yields the full vertex form factors

$$\hat{F}_L^S = \frac{1}{\sqrt{2}} \Delta_u' Y_d [Z_R^{2k} - Z_R^{1k} \tan\beta] \approx -\frac{1}{\sqrt{2}} \Delta_u' Y_d Z_R^{1k} \tan\beta, \tag{32}$$

$$\hat{F}_L^P = \frac{1}{\sqrt{2}} \Delta_u' Y_d [Z_H^{2k} + Z_H^{1k} \tan\beta] \approx \frac{1}{\sqrt{2}} \Delta_u' Y_d Z_H^{1k} \tan\beta$$

(right form factors are given by the Hermitean conjugation; they involve Y_d^I and are therefore subleading).

Detailed comparison of the above simplified calculation with the standard diagramatic approach (in which one computes both, the self-energy corrections, and one particle irreducible the 1PI vertex diagrams, in the phase in which the electroweak symmetry is broken) reveals that the dominant contributions given by Eqs. (32) to the form factors arise only from the self-energy diagrams (the 1PI vertex corrections contain one power of $\tan\beta$ less). Moreover, the com-

[7] Strictly speaking, Eq. (27) must hold only for off-diagonal elements; for $A=B$, the relation $m_{d_A} = -Y_d^A v_1/\sqrt{2}$ is corrected, but the net result is that in Eq. (28) $Y_d^A \equiv -\sqrt{2} m_{d_A}/v_1$ again.

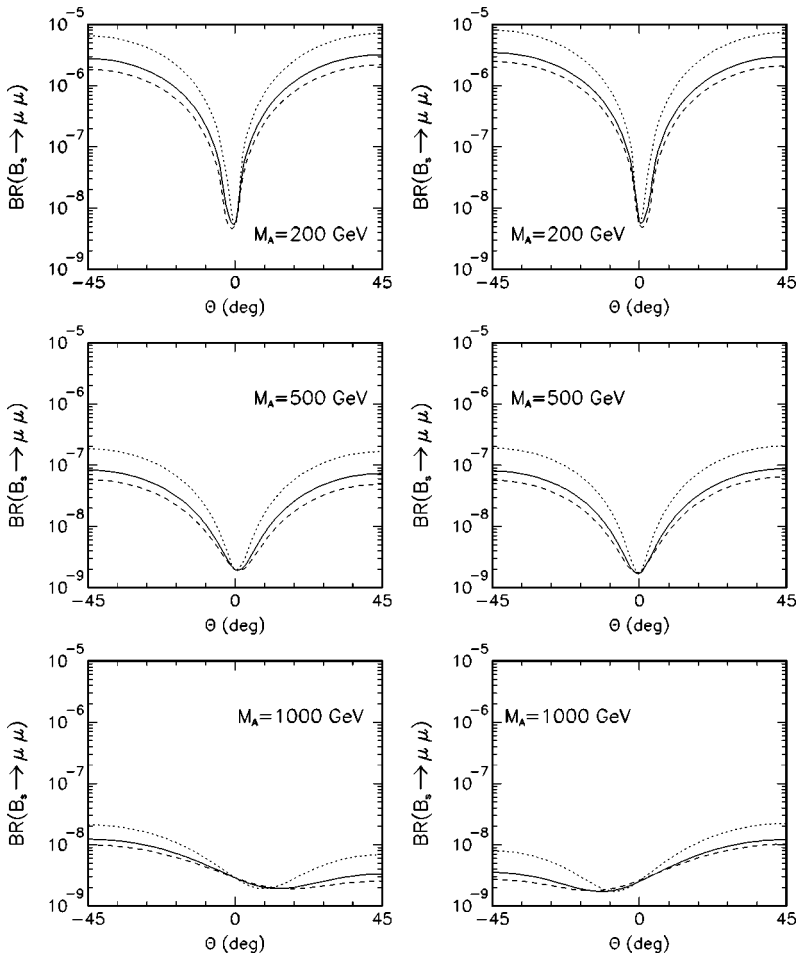

FIG. 3. BR($B^0_s\to\mu^-\mu^+$) as a function of the top squark mixing angle θ_t for $\tan\beta=50$, the lighter chargino mass 100 GeV and different values of M_A. Solid, dashed and dotted lines correspond to ($M_{\tilde{t}_2}$,$M_{\tilde{t}_1}$) equal (240,500), (400,700) and (300,850) GeV, respectively. In the left (right) panels $M_2/\mu=10(-1)$, where M_2 is the usual $SU(2)$ gaugino mass parameter.

parison shows that one should replace A_t by $\tilde{A}_t\equiv A_t+\mu\cot\beta$, $M_{\tilde{t}_L}$, $M_{\tilde{t}_R}$ with the true mass eigenstates $M_{\tilde{t}_1}$, $M_{\tilde{t}_2}$ and justifies the replacement of $\pm\mu$ by the mass of the lighter chargino.

Using Eq. (32) we get

$$a=\frac{f_B}{4}\frac{1}{16\pi^2}\lambda_{tI}\frac{2m_l}{M_W^2}\left(\frac{e}{s_W}\right)^4\left[Y(x_t)-\frac{M_B^2}{8M_W^2}\tan^2\beta\frac{\log r}{r-1}\pm\frac{M_B^2}{8M_W^2}\frac{m_t^2}{M_A^2}\tan^3\beta\tilde{A}_t m_{C_1}C_0\right], \tag{33}$$

$$b=\frac{f_B}{4}\frac{1}{16\pi^2}\lambda_{tI}\frac{2m_l}{M_W^2}\left(\frac{e}{s_W}\right)^4\left[-\frac{M_B^2}{8M_W}\tan^2\beta\frac{\log r}{r-1}\pm\frac{M_B^2}{8M_W^2}\frac{m_t^2}{M_A^2}\tan^3\beta\tilde{A}_t m_{C_1}C_0\right]. \tag{34}$$

Knowing that $Y(x_t)\approx 1$, these formulas allow for a quick estimate of the effects. It is important to note that the contribution of charginos to the rate grows as $\tan^6\beta$ and therefore can be much larger than the contribution of the Higgs sector.

Figure 3 shows the dependence of the full branching ratio BR($B^0_s\to\mu^-\mu^+$), including the SM, Higgs boson and chargino contributions, on the mixing angle of the top squarks for some values of the other MSSM parameters. The minimum around $\theta_t\approx 0$ corresponding to $\tilde{A}_t\approx 0$ is clearly seen. Incidentally, this plot also supports the replacement of μ by $\pm m_{C_1}$ in Eq. (31), because very similarly (up to a reflection $\theta_t\to-\theta_t$ which follows from different signs of μ) looking curves in the left and right panels have the same m_{C_1} but distinctly different μ. Another important feature of the chargino contribution is that it does not vanish if all sparticle mass parameters are scaled uniformly: $M_{\tilde{t}_i}\to\lambda M_{\tilde{t}_i}$, $m_{C_i}\to\lambda m_{C_i}$, $\mu\to\lambda\mu$, $A_t\to\lambda A_t$. This is clear from the fact that in such a case $C_0\to\lambda^{-2}C_0$. This is illustrated in Fig. 4 which shows BR($B^0_s\to\mu^-\mu^+$) as a function of the lighter chargino mass for ($M_{\tilde{t}_2}$,$M_{\tilde{t}_1}$) equal to (m_C,$3m_C$) and $\theta_t=10°$ (solid lines), (m_C,$3m_C$) and $\theta_t=30°$ (dashed lines), ($3m_C$,$5m_C$) and $\theta_t=10°$ (dotted lines) and ($3m_C$,$5m_C$) and $\theta_t=30°$ (dash-dotted lines). In fact, keeping the stop mixing angle fixed requires that $\tilde{A}_t$ scales as λ^2 rather than as λ, which explains the growth of the rates with m_{C_1} in Fig. 4.

To check the correlation of the prediction for BR($B^0_s\to\mu^-\mu^+$) with the results for BR($B\to X_s\gamma$), we have performed scans over the relevant parameter space of the MSSM. We took the following ranges: $100<m_{C_1}<1000$ GeV, $0.1<|M_2/\mu|<10$, $1<M_{\tilde{t}_2}/m_{C_1}<10$, $1<M_{\tilde{t}_1}/M_{\tilde{t}_2}$

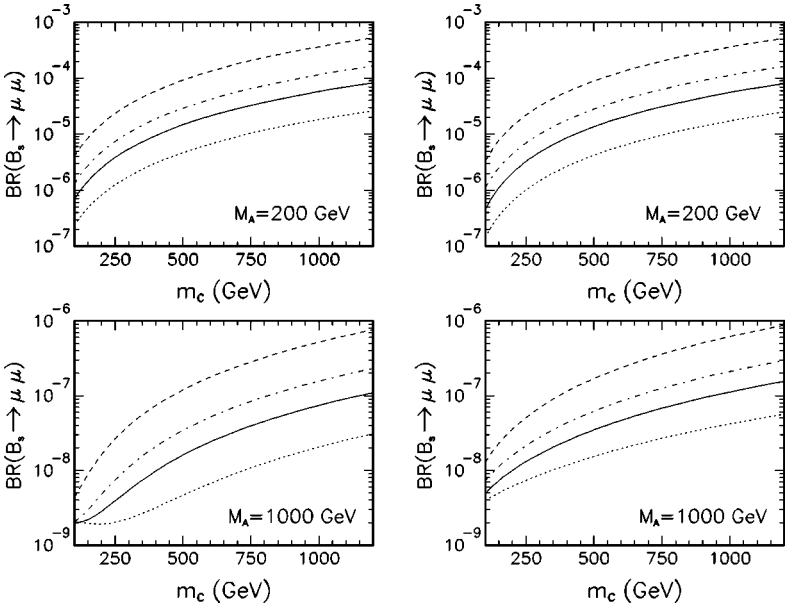

FIG. 4. BR($B_s^0 \to \mu^- \mu^+$) as a function of the lighter chargino mass for $\tan\beta = 50$, $M_A = 200$ and 1000 GeV. Solid (dashed) lines correspond to ($M_{\tilde{t}_2}, M_{\tilde{t}_1}$) equal to ($m_{C_1}, 3m_{C_1}$) and the stop mixing angle $\theta_t = 10°$ (30°), whereas dotted (dash-dotted) lines to ($3m_{C_1}, 5m_{C_1}$) and $\theta_t = 10°$ (30°), respectively. In the left (right) panels $M_2/\mu = 10(-1)$.

<5 and $-60° < \theta_t < 60°$ and rejected points for which $\Delta\rho_{\rm squarks} > 6 \times 10^{-4}$ and $M_h < 107$ GeV. For calculating BR($B \to X_s\gamma$) we have used the routine based on Refs. [20,21] including the next-to-leading order (NLO) matching conditions at the scale M_Z for the top and charged Higgs contribution, as in Refs. [22,23], and only the LO ones for the supersymmetric contribution [24,5]. We have not used the available NLO matching conditions for the supersymmetric particles since they are computed under the specific assumptions about the sparticle spectrum, not necessarily satisfied in the scan and, moreover, not valid for large values of $\tan\beta$. The theoretical uncertainty is taken into account by computing the rate for $\mu_h = 2.4$ and 9.6 GeV and then by shifting its larger (smaller) value upward (downward) by the added in quadratures errors related to the uncertainties in α_s, m_b, m_c/m_b, $|V_{tb}V_{ts}^\star/V_{cb}|^2$, and higher order electroweak corrections; we do not take into account the variation of the scale μ_W. For a given set of the parameters of the MSSM the BR($B \to X_s\gamma$) value shown in Fig. 5 corresponds to the lowest (highest) edge of the resulting band of theoretical predictions, if the whole band is above (below) the range allowed by CLEO [10], and to the central point of the overlap of the theoretical and CLEO bands in the case such an overlap exists.

In the case of the $B_s^0 \to \mu^- \mu^+$ decay, the results of the scans, shown in Figs. 5(a)–5(d), demonstrate that the the CLEO result for BR($B \to X_s\gamma$) does not eliminate the points corresponding to the largest values of BR($B_s^0 \to \mu^- \mu^+$) and even does not exhibit any definite correlation between the two rates, especially for those points for which BR($B_s^0 \to \mu^- \mu^+$) is very large. This is mainly due to the fact that the (LO) chargino contribution to BR($B \to X_s\gamma$) decreases with growing sparticle masses, whereas its contribution to BR($B_s^0 \to \mu^- \mu^+$) does not. This allows to hope that even the

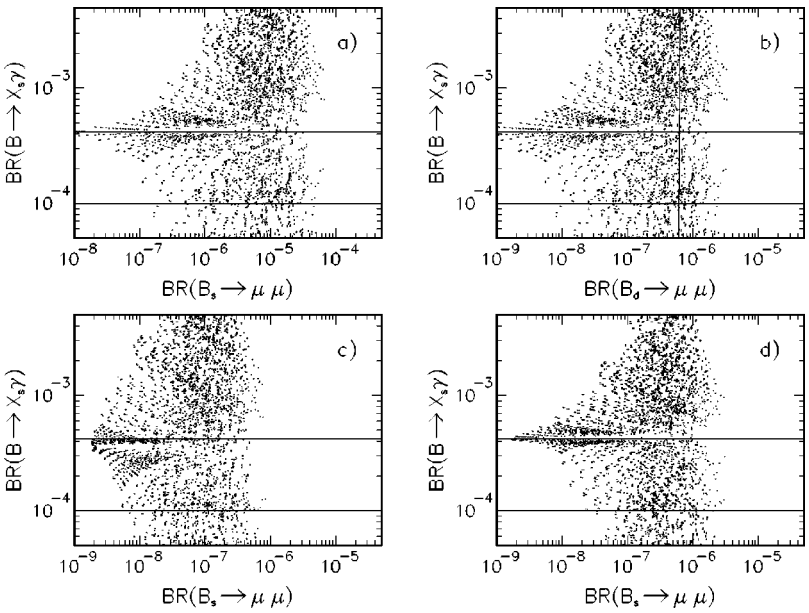

FIG. 5. BR($B \to X_s\gamma$) vs BR($B_{s(d)}^0 \to \mu^- \mu^+$) for $\tan\beta = 50$, $M_A = 200$ GeV in panels (a) and (b), $\tan\beta = 50$, $M_A = 600$ GeV in panel (c) and $\tan\beta = 30$, $M_A = 200$ in panel (d). Limits from CLEO on BR($B \to X_s\gamma$) and on BR($B_d^0 \to \mu^- \mu^+$) are also shown by solid lines.

full NLO computation of BR($B\to X_s\gamma$) will not change this picture qualitatively. In the case of the $B^0_d\to\mu^-\mu^+$ decay, for each set of the MSSM parameters, the relevant element V_{td} should be determined from the prediction for the ϵ_K parameter and B^0_d-$\overline{B}^0_d$ mass difference by consistently including all supersymmetric contributions. Such an analysis is beyond the scope of the present paper and we limit ourselves to the following remarks. In Fig. 5(b), we have used the SM value $|V_{td}|\approx 0.008$, which means that the values of BR($B^0_d\to\mu^-\mu^+$) shown in Fig. 5(b) can, in principle, be increased (or decreased) at most by a factor of ≈ 3 when this element is determined properly. However, as follows from Fig. 4, the largest values of BR($B^0_d\to\mu^-\mu^+$) are obtained for heavy charginos and/or stops, which means that in those cases the supersymmetric contribution to the ϵ_K parameter and B^0_d-$\overline{B}^0_d$ mass difference is small and the SM value of $|V_{td}|$ we have used cannot deviate too much from its correct value. One can therefore conclude that Fig. 5 demonstrates that the present CLEO bound BR($B^0_d\to\mu^-\mu^+$)$<6.2\times10^{-7}$ (shown in the upper-right plot by the vertical solid line) already puts some weak constraints on the MSSM parameter space in the case of large $\tan\beta\sim m_t/m_b$ and $M_A\lesssim 300$ GeV.

V. FLAVOR CHANGING INDUCED BY SFERMION MASS MATRICES

Up to now we have assumed that the fermion and sfermion mass matrices are flavor diagonal in the same basis (the so-called super-CKM basis). In this section, we consider the effects of nondiagonal entries in the sfermion mass matrices. It is customary to parametrize such nondiagonal entries by the so-called dimensionless mass insertions [2,3],

$$(\delta^K_{XY})^{IJ}\equiv\frac{(\Delta\mathcal{M}^2_K)^{IJ}_{XY}}{\sqrt{(\mathcal{M}^2_K)^{II}_{XX}(\mathcal{M}^2_K)^{JJ}_{YY}}},\tag{35}$$

where $X,Y=L,R$, $K=u,d,l$, $(\mathcal{M}^2_K)^{II}_{XX}$ are the diagonal elements of the XX blocks of the full mass squared matrices and $(\Delta\mathcal{M}^2_K)^{IJ}_{XY}$ are the off-diagonal entries of the XY blocks. Most of these insertions are bounded by the existing experimental data (for review, see Refs. [2,3]). In the case of the $B^0\to\overline{l^B}l^A$ decay, the relevant insertions are $(\delta^l_{XY})^{AB}$ and $(\delta^d_{XY})^{I3}$, $I=1,2$.

The first interesting point is to check the effects of the slepton mass insertions which are the only source of the decays $B^0\to\overline{l}\overline{l}'$ (through the box diagrams with charginos in the loop). Very strong bounds from nonobservation of the transition $\mu\to e\gamma$ exist only on the $(\delta^l_{LR})^{12}$ insertions [2], whereas in the case of the $B^0\to\overline{l}\overline{l}'$ decay most important are the insertions δ^l_{LL} on which the bounds are weaker.[8] Taking $m_{C_1}=100$ GeV, light top squark $M_{\tilde{t}_2}\approx 100$ GeV and adjusting the slepton sector mass parameters so to keep $M_{\tilde{l}}\gtrsim 90$ GeV, $M_{\tilde{\nu}}\gtrsim 50$ for $(\delta^l_{LL})^{13(23)}\approx 0.9$, we get

$$\begin{aligned}\mathrm{BR}(B^0_s\to\overline{l}\overline{l}')&\lesssim 1.6\times10^{-11},\\ \mathrm{BR}(B^0_d\to\overline{l}\overline{l}')&\lesssim 3.8\times10^{-13},\end{aligned}\tag{36}$$

where $ll'=e\tau$ or $\mu\tau$. (The largest rates are obtained for $|M_2/\mu|\lesssim 1$ and small stop mixing angle θ_t; the result scale approximately as $|\delta^l_{LL}|^2$.) For other parameters (heavier stops and charginos) branching fractions for these processes are, of course, smaller.

We now discuss the effects of the flavor nondiagonal mass insertions in the down-type squark mass matrix and return to the $\overline{l}\overline{l}$ final states. The approximate formulas accounting for the effects of the insertions $(\delta^d_{XY})^{IJ}$ are easily derived in the so-called mass insertion method [2,3] in which flavor off-diagonal elements of the sfermion mass squared matrices are treated as additional interactions. Usually, the linear approximation in $(\delta^d_{XY})^{IJ}$ is sufficient to account for the results obtained with the full diagramatic calculation. In the case of a nonzero $(\delta^d_{XY})^{I3}$ insertion, the dominant contribution is expected to come from the diagrams involving gluinos, due to their strong coupling, $g_s=\sqrt{4\pi\alpha_s}$, to quarks and squarks.[9] (This expectation is confirmed by the numerical computation in which all one-loop contributions are taken into account.) Since at one-loop there are no box diagrams with gluinos, we are left only with the Z^0 and neutral Higgs boson penguin diagrams. As previously, the latter type of penguin diagrams is important only for large values of $\tan\beta$. Another important remark is that because the change of flavor in the gluino diagrams does not originate from the CKM mass matrix, the rates of the B^0_d decays need not be suppressed compared to the rates of the B^0_s decays.

For $\tan\beta$ values not too large, only the Z^0 penguin contribution can be important. Direct computation shows, however, that in the formula (11) terms linear in the mass insertions $(\delta^d_{LL(RR)})^{I3}$ cancel out completely between the self-energy Σ^V_X and the proper vertex correction F^V_X ($X=L,R$). Because of that, the effects of the nonzero $(\delta^d_{LL(RR)})^{I3}$ mass insertions, even taking into account their quadratic and higher contributions in gluino exchanges as well as neutralino diagrams, are small for $\tan\beta$ values for which the neutral Higgs boson penguin graphs are negligible. Larger effects could come only from nonzero $(\delta^d_{LR})^{I3}$ mass insertions which, however, are strongly constrained [2,3]: $|(\delta^d_{LR})^{13}|<0.07(m_{max}/1\ \ \mathrm{TeV})$, $|(\delta^d_{LR})^{23}|<0.03(m_{max}/1$

[8]Reference [2] gives $(\delta^l_{LL})^{12}<0.2(M_{\tilde{\nu}}/0.5\ \mathrm{TeV})^2$, $(\delta^l_{LL})^{13}<700(M_{\tilde{\nu}}/0.5\ \mathrm{TeV})^2$ and $(\delta^l_{LL})^{23}<100(M_{\tilde{\nu}}/0.5\ \mathrm{TeV})^2$, which in most cases are superseded by $\delta^l_{LL}\lesssim 1$—the limit in which one of the sneutrinos becomes tachionic.

[9]For nonzero $(\delta^d_{XY})^{I3}$ insertion also neutralinos contribute; moreover, a nonzero $(\delta^d_{LL})^{I3}$ insertion induces, via the CKM matrix (see, e.g., Refs. [3,12]), nonzero $(\delta^u_{LL})^{I3}$ insertions which affect, in principle, the chargino contribution. Both these effects are small but are taken into account in our numerical code.

TeV) [where $m_{max} \equiv (\max(M_{sq}, m_{\tilde{g}}))$]. Respecting these constraints, BR($B_s^0 \to \mu^- \mu^+$) (BR($B_d^0 \to \mu^- \mu^+$)) remains of order 4×10^{-9} (10^{-10}).

In the case of large $\tan\beta$, we have to compute in the linear approximation in the mass insertions both the scalar parts of the self-energies and the 1PI vertex corrections to the couplings $\bar{d}_J d_I S^0(P^0)$. For the self-energies we get

$$\Sigma_L^S = -\frac{1}{16\pi^2}\frac{8}{3} g_s^2 m_{\tilde{g}} \{ (\Delta \mathcal{M}_D^2)_{LR}^{IJ} C_0(m_{\tilde{g}}^2, M_D^2, M_D^2) - (\Delta \mathcal{M}_D^2)_{LL}^{IJ} m_b (A_b + \mu \tan\beta) D_0(m_{\tilde{g}}^2, M_D^2, M_D^2, M_D^2) \}, \tag{37}$$

where D_0 is the standard four-point function

$$D_0(a,b,c,d) = \frac{1}{a-b}[C_0(a,c,d) - C_0(b,c,d)], \tag{38}$$

$m_{\tilde{g}}$ is the gluino mass and M_D is the average mass of the two bottom squarks. A similar formula is obtained for Σ_R^S with the replacement $(\Delta \mathcal{M}_D^2)_{LL} \to -(\Delta \mathcal{M}_D^2)_{RR}$.

In the same approximation, for the vertex correction $\bar{d}_J d_I P^0$ we get

$$F_L^P = \frac{1}{16\pi^2}\frac{8}{3} g_s^2 m_{\tilde{g}} \Bigg\{ \frac{1}{v_1} Z_H^{1k} (\Delta \mathcal{M}_D^2)_{LR}^{IJ} C_0(m_{\tilde{g}}^2, M_D^2, M_D^2) + \frac{e}{2 s_W}\frac{\mu}{M_W} (m_{d_I} (\Delta \mathcal{M}_D^2)_{RR}^{IJ} + (\Delta \mathcal{M}_D^2)_{LL}^{IJ} m_{d_J}) \times Z_H^{2k} \tan\beta D_0(m_{\tilde{g}}^2, M_D^2, M_D^2, M_D^2) - Z_H^{1k} \tan\beta \frac{e}{2 s_W M_W} A_b (m_{d_I} (\Delta \mathcal{M}_D^2)_{RR}^{IJ} + m_{d_J} (\Delta \mathcal{M}_D^2)_{LL}^{IJ}) D_0(m_{\tilde{g}}^2, M_D^2, M_D^2, M_D^2) \Bigg\}, \tag{39}$$

where for the three-linear soft term we have used $A_D^{II} \equiv Y_d^I A_b$. F_R^P is similar, with $(\Delta \mathcal{M}_D^2)_{LL}^{IJ} \leftrightarrow -(\Delta \mathcal{M}_D^2)_{RR}^{IJ}$. Combining Eqs. (39) and (37) according to Eq. (13), we see that $(\Delta \mathcal{M}_D^2)_{RL}^{IJ}$ cancels out. Moreover, since the CP-odd scalar A^0, whose coupling to leptons is enhanced, corresponds to $k=1$ and $Z_H^{21} = \cos\beta \approx 0$, the second line in Eq. (39) is suppressed compared to the third one. Therefore, we can write

$$\hat{F}_L^P \approx -\frac{1}{16\pi^2}\frac{8}{3} g_s^2 \frac{e}{2 s_W}\frac{m_b}{M_W}\tan^2\beta \times \mu (\Delta \mathcal{M}_D^2)_{LL}^{IJ} m_{\tilde{g}} D_0(m_{\tilde{g}}^2, M_D^2, M_D^2, M_D^2), \tag{40}$$

where we have retained only $(\Delta \mathcal{M}_D^2)_{LL}^{IJ}$ which in $\hat{F}_L^P$ is multiplied by $m_{d_J} = m_b$ and neglected $(\Delta \mathcal{M}_D^2)_{RR}^{IJ}$ which is multiplied by m_{d_I} (in $\hat{F}_R^P$ it is the other way around). Similar calculation leads to

$$\hat{F}_L^S \approx \frac{1}{16\pi^2}\frac{8}{3} g_s^2 \frac{e}{2 s_W}\frac{m_b}{M_W}\tan^2\beta \times \mu (\Delta \mathcal{M}_D^2)_{LL}^{IJ} m_{\tilde{g}} D_0(m_{\tilde{g}}^2, M_D^2, M_D^2, M_D^2). \tag{41}$$

Computing the relevant Wilson coefficients, we finally find for the coefficients a and b

$$a = \frac{1}{16\pi^2}\frac{f_B}{2}\frac{m_l}{M_W^2}\left(\frac{e}{s_W}\right)^4 \lambda_{tI} \times \Bigg[Y(x_t) - \frac{8}{3} g_s^2 \left(\frac{s_W}{e}\right)^2 \frac{M_B^2}{M_{A^0}^2}\frac{(\delta_{LL}^d)^{I3}}{\lambda_{tI}} \times \tan^3\beta m_{\tilde{g}} \mu M_D^2 D_0(m_{\tilde{g}}^2, M_D^2, M_D^2, M_D^2) \Bigg], \tag{42}$$

$$b = \frac{1}{16\pi^2}\frac{f_B}{2}\frac{m_l}{M_W^2}\left(\frac{e}{s_W}\right)^4 \lambda_{tI} \times \Bigg[-\frac{8}{3} g_s^2 \left(\frac{s_W}{e}\right)^2 \frac{M_B^2}{M_{A^0}^2}\frac{(\delta_{LL}^d)^{I3}}{\lambda_{tI}} \times \tan^3\beta m_{\tilde{g}} \mu M_D^2 D_0(m_{\tilde{g}}^2, M_D^2, M_D^2, M_D^2) \Bigg], \tag{43}$$

in which we have also displayed the SM contribution to allow for easy estimate of the magnitude of the gluino contribution. It is essential that the dominant effect is due to the LL insertion and not the LR one which is much more strongly constrained [2,3]. Similarly as in the case of the chargino contribution through the neutral Higgs boson penguin graphs, the gluino (and neutralino) contribution is also proportional to $\tan^6\beta$ and does not vanish when all SUSY mass parameters are uniformly scaled up (provided the dimensionless mass insertion is kept fixed). Figure 6 shows the result of the full diagramatic computation of the SM and gluino exchange contributions to BR($B_s^0 \to \mu^- \mu^+$) as a function of the μ parameter for $(\delta_{LL}^d)^{23} = 0.1$ and $\tan\beta = 50$, $M_A = 200$ GeV. The minimum for $\mu = 0$ is clearly seen. The gluino contribution scales approximately as $|(\delta_{LL}^d)^{23}|^2$.

Figure 7 shows the results of the general scan over the MSSM parameter space in the form of the scatter plot BR($B \to X_s \gamma$) vs BR($B_s^0 \to \mu^- \mu^+$) for $(\delta_{LL}^d)^{23} = 0.1$ and vs BR($B_d^0 \to \mu^- \mu^+$) for $(\delta_{LL}^d)^{13} = 0.05$. The parameters have been varied in the following ranges: $100 < m_{C_1} < 600$ GeV, $0.1 < |M_2/\mu| < 5$, $m_{\tilde{g}} = 3 M_2$, $-60° < \theta_t < 60°$, $A_b = A_t$, $0.5 < M_{\tilde{t}_2}/m_{C_1} < 1.5$, $1 < M_{\tilde{t}_1}/M_{\tilde{t}_2} < 5$, $0.25 < (m_D^2)_{33}/m_{\tilde{g}}^2 < 2.25$. For other entries of the squark mass matrices we took $(m_X^2)_{KK} = (m_D^2)_{33}$. All points for which $M_h < 107$ GeV, $\Delta\rho_{squark} > 6 \times 10^{-4}$ (as well as points with too light stops) have been rejected. Results for $(\delta_{RR}^d)^{I3}$ are similar.

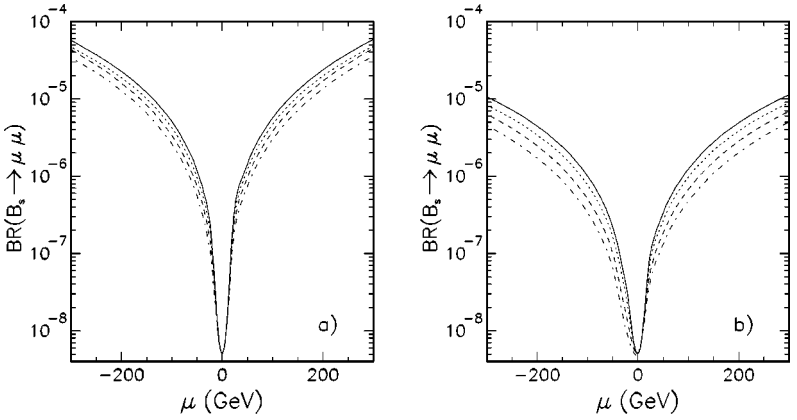

FIG. 6. BR($B^0_s\to\mu^-\mu^+$) for $\tan\beta=50$, $M_A=200$ GeV and $(\delta^d_{LL})^{23}=0.1$ as a function of the μ parameter. In the left panel $(m_{\tilde g},A_t=A_b)$ equals (300,0) GeV (solid line), (300,250) GeV (dashed line), (800,0) GeV (dotted line) and (800,250) GeV (dash-dotted line); $(m^2_Q)_{33}=(500\ \text{GeV})^2$, $(m^2_U)_{33}=(m^2_D)_{33}=(300\ \text{GeV})^2$, $(m^2_X)_{KK}=(600\ \text{GeV})^2$ for $K\neq 3$. In the right panel $(m_{\tilde g},A_t=A_b)$ equals: (800,0) GeV (solid line), (800,450) GeV (dashed line), (1500,0) GeV (dotted line) and (1500,450) GeV (dash-dotted line); $(m^2_Q)_{33}=(900\ \text{GeV})^2$, $(m^2_U)_{33}=(m^2_D)_{33}=(700\ \text{GeV})^2$, $(m^2_X)_{KK}=1000\ \text{GeV}^2$ for $K\neq 3$.

In agreement with the bounds given in Refs. [2,3], the measured by CLEO [10] BR($B\to X_s\gamma$) does not constrain the rate of the BR($B^0_s\to\mu^-\mu^+$) decay (nor does it exhibit any particular correlation with the latter), and the latter can attain values of the order of 10^{-4}, respecting all the relevant phenomenological constraints. As expected, whenever the gluino contribution is dominant, the rates of the $B^0_s\to\mu^-\mu^+$ and $B^0_d\to\mu^-\mu^+$ decays are comparable, which means that BR($B^0_d\to\mu^-\mu^+$) can also be as large as 10^{-4} for $(\delta^d_{LL})^{13}=0.1$ [in the plot, we took $(\delta^d_{LL})^{13}=0.05$ in order to satisfy the bound $(\delta^d_{LL(RR)})^{13}<0.2(m_{max}/1\ \text{TeV})$ [2,3] for almost all points in the scan; however, the biggest effects are for m_{max} large in which $(\delta^d_{LL(RR)})^{13}$ can be larger]. It follows that for such values of the MSSM parameters, the current CLEO bound, BR($B^0_d\to\mu^-\mu^+$)$<6.2\times10^{-7}$ [11], puts constraints on $(\delta^d_{LL(RR)})^{13}$ which are much stronger than the ones given in Refs. [2,3].

VI. CONCLUSIONS

We have performed a complete one loop diagramatic calculation of the decay rate of the $B^0_{s(d)}$ mesons into charged leptons. Both possible sources of the FCNC processes, the CKM mixing matrix and the off-diagonal entries of the sfermion mass matrices, have been considered. For values of $\tan\beta$, in which the neutral Higgs boson penguin graphs are negligible, the rates of these decays in the MSSM remain of the order of the SM prediction.

Large enhancement of the SM prediction can occur for $\tan\beta\gg1$, provided the additional Higgs bosons predicted by the MSSM are not too heavy (all the large contributions behave as $1/M_A^2$, where M_A is the mass of the CP-odd neutral Higgs boson). The contribution of the Higgs sector grows like $\tan^4\beta$ and can give BR($B^0_s\to\mu^-\mu^+$)$\sim2\times10^{-8}$ for $\tan\beta\sim m_t/m_b$. Dominant effects of the chargino sector grow as $\tan^6\beta$ and depend strongly on the top squark mixing. For $\tan\beta\sim m_t/m_b$ and substantial mixing of the top squarks they can give BR($B^0_{s(d)}\to\mu^-\mu^+$) up to $5\times10^{-5}(10^{-6})$, respecting other phenomenological constraints including the measurement of BR($B\to X_s\gamma$). Large effects, growing as $\tan^6\beta$ and exhibiting strong dependence on the μ parameter, can be also induced by the off-diagonal elements of the down-type squark mass matrix. As we have shown, BR($B^0_{s(d)}\to\mu^-\mu^+$) is sensitive to the 23 (13) off-

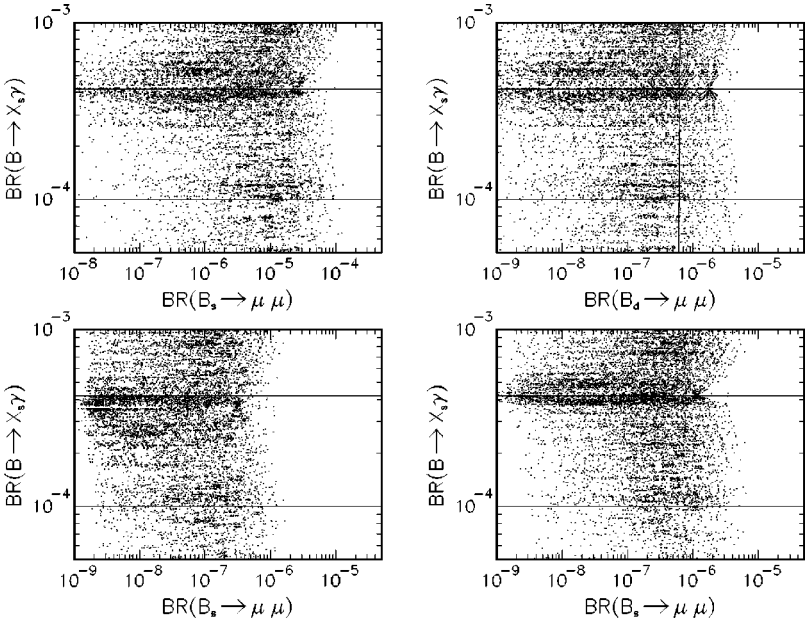

FIG. 7. BR($B\to X_s\gamma$) vs BR($B^0_s\to\mu^-\mu^+$) [with $(\delta^d_{LL})^{23}=0.1$] and BR($B^0_d\to\mu^-\mu^+$) [with $(\delta^d_{LL})^{13}=0.05$] for $\tan\beta=50$, $M_A=200$ GeV in panels (a) and (b), $\tan\beta=50$, $M_A=600$ GeV in panel (c) and $\tan\beta=30$, $M_A=200$ in panel (d). Limits from CLEO on BR($B\to X_s\gamma$) and BR($B^0_d\to\mu^-\mu^+$) are also shown by solid lines.

diagonal entries of the LL and RR blocks of these matrices, which are not so strongly constrained by BR($B \to X_s \gamma$). For $\tan\beta \sim m_t/m_b$ and $M_A \lesssim 200$ GeV these effects can easily give BR($B_s^0 \to \mu^- \mu^+$) larger than 10^{-4}. It is also interesting that even for $BR(B_d^0 \to \mu^- \mu^+)$ these effects can be so large that they could exceed the present CLEO limit [11] which, therefore, already now puts constraints on the MSSM parameter space.

Finally, it is important to stress that both types of effects growing as $\tan^6\beta$ do not necessarily decrease as sparticles become heavy. However, they are sensitive to the mass scale of the extended Higgs sector. Thus large deviation from the SM prediction observed in these decays, apart from being a signal of supersymmetry, would have important implications for the Higgs search at the LHC.

ACKNOWLEDGMENTS

P.H. Ch. would like to thank S. Pokorski for useful discussion. His work was partly supported by the Polish State Committee for Scientific Research Grant No. 2 P03B 052 16 for 1999-2000.

[1] F. M. Borzumati and C. Greub, Phys. Rev. D **58**, 074004 (1998); **59**, 057501 (1999).
[2] F. Gabbiani, E. Gabrielli, A. Masiero, and L. Silvestrini, Nucl. Phys. **B477**, 321 (1996).
[3] M. Misiak, S. Pokorski, and J. Rosiek, in *Heavy Flavors II*, edited by A. J. Buras and M. Lindner (World Scientific, Singapore, 1998), hep-ph/9703442.
[4] A. Brignole, F. Feruglio, and F. Zwirner, Z. Phys. C **71**, 679 (1996).
[5] S. Bertolini, F. M. Borzumati, A. Masiero, and G. Ridolfi, Nucl. Phys. **B353**, 591 (1991).
[6] N. Oshimo, Nucl. Phys. **B404**, 20 (1993); C.-S. Huang and Q.-S. Yan, Phys. Lett. B **442**, 3811 (1998); C.-S. Huang, W. Liao, and Q.-S. Yan, Phys. Rev. D **59**, 011701 (1999); S. R. Chaudhury and N. Gaur, Phys. Lett. B **451**, 86 (1999); C.-S. Huang, W. Liao, Q.-S. Yan, and S.-H. Zhu, hep-ph/0006250.
[7] K. Babu and C. Kolda, Phys. Rev. Lett. **84**, 228 (2000).
[8] J. L. Hewett, S. Nandi, and T. G. Rizzo, Phys. Rev. D **39**, 250 (1989).
[9] C. Hamzaoui, M. Pospelov, and M. Toharia, Phys. Rev. D **59**, 095005 (1999).
[10] The CLEO Collaboration, Paper ICHEP98 1011 submitted to the XXIX International Conference on High Energy Physics, Vancouver, British Columbia, Canada (CLEO CONF98-17).
[11] CLEO Collaboration, T. Włodek, talk at the American Physical Society Meeting, Long Beach, 2000.
[12] J. Rosiek, Phys. Rev. D **41**, 3464 (1990); hep-ph/9511250.
[13] G. Buchalla and A. J. Buras, Nucl. Phys. **B400**, 225 (1993).
[14] A. J. Buras, in *Probing the Standard Model of Particle Interactions*, edited by F. David and R. Gupta (Elsevier Science, New York), hep-ph/9806471.
[15] G. Buchalla, A. J. Buras, and M. K. Harlander, Nucl. Phys. **B349**, 1 (1991); M. Misiak and J. Urban, Phys. Lett. B **451**, 161 (1999).
[16] H. Logan and U. Nierste, Nucl. Phys. **B586**, 39 (2000).
[17] W. Skiba and J. Kalinowski, Nucl. Phys. **B404**, 3 (1993).
[18] P. H. Chankowski and S. Pokorski, in *Perspectives on Supersymmetry*, edited by G. L. Kane (World Scientific, Singapore, 1998), hep-ph/9707497; P. H. Chankowski, *Proceedings of the Workshop Quantum Effects in the MSSM*, Barcelona, 1997, edited by J. Sòla (World Scientific, Singapore, 1998), hep-ph/9711470.
[19] P. H. Chankowski and S. Pokorski, Nucl. Phys. **B475**, 3 (1996).
[20] K. Chetyrkin, M. Misiak, and M. Münz, Phys. Lett. B **400**, 206 (1997).
[21] A. Czarnecki and W. A. Marciano, Phys. Rev. Lett. **81**, 277 (1998); A. Kagan and M. Neubert, Eur. Phys. J. C **7**, 5 (1999).
[22] K. Adel and Y. P. Yao, Phys. Rev. D **49**, 4945 (1994); C. Greub, T. Hurth, and D. Wyler, Phys. Lett. B **380**, 385 (1996); Phys. Rev. D **54**, 3350 (1996).
[23] M. Ciuchini, G. Degrassi, P. Gambino, and G.-F. Giudice, Nucl. Phys. **B527**, 21 (1998); P. Ciafaloni, A. Romanino, and A. Strumia, *ibid.* **B524**, 361 (1998).
[24] R. Barbieri and G.-F. Giudice, Phys. Lett. B **309**, 86 (1993).